

MTech_Thesis-2.pdf

 Indian Statistical Institute

Document Details

Submission ID

trn:oid:::3618:100348094

Submission Date

Jun 11, 2025, 2:58 PM GMT+5:30

Download Date

Jun 11, 2025, 3:01 PM GMT+5:30

File Name

MTech_Thesis-2.pdf

File Size

504.8 KB

31 Pages

6,486 Words

30,284 Characters

10% Overall Similarity

The combined total of all matches, including overlapping sources, for each database.

Filtered from the Report

- Bibliography

Exclusions





- 15 Excluded Matches

Custom Section Exclusions




{titlesCount} Section Titles, {keywordsCount} Keywords

Section title	No. of Section Starters	Section Starters
"isi"	2	Indian statistical institute kolkata

Match Groups


-  **62 Not Cited or Quoted 9%**
Matches with neither in-text citation nor quotation marks
-  **5 Missing Quotations 1%**
Matches that are still very similar to source material
-  **0 Missing Citation 0%**
Matches that have quotation marks, but no in-text citation
-  **0 Cited and Quoted 0%**
Matches with in-text citation present, but no quotation marks

Top Sources

- 7%  Internet sources
- 7%  Publications
- 0%  Submitted works (Student Papers)

Integrity Flags

1 Integrity Flag for Review

-  **Replaced Characters**
74 suspect characters on 9 pages
Letters are swapped with similar characters from another alphabet.

Our system's algorithms look deeply at a document for any inconsistencies that would set it apart from a normal submission. If we notice something strange, we flag it for you to review.

A Flag is not necessarily an indicator of a problem. However, we'd recommend you focus your attention there for further review.

Match Groups

- 62 Not Cited or Quoted 9%**
Matches with neither in-text citation nor quotation marks
- 5 Missing Quotations 1%**
Matches that are still very similar to source material
- 0 Missing Citation 0%**
Matches that have quotation marks, but no in-text citation
- 0 Cited and Quoted 0%**
Matches with in-text citation present, but no quotation marks

Top Sources

- 7% Internet sources
- 7% Publications
- 0% Submitted works (Student Papers)

Top Sources

The sources with the highest number of matches within the submission. Overlapping sources will not be displayed.

1	Internet	trepo.tuni.fi	2%
2	Internet	dokumen.pub	<1%
3	Internet	arxiv.org	<1%
4	Internet	export.arxiv.org	<1%
5	Publication	Matthew A. Carlton, Jay L. Devore. "Probability with Applications in Engineering, S...	<1%
6	Internet	ebin.pub	<1%
7	Publication	Margarita Gapeyenko, Dmitri Moltchanov, Sergey Andreev, Robert W. Heath. "Lin...	<1%
8	Internet	users.ece.utexas.edu	<1%
9	Internet	researchrepository.wvu.edu	<1%
10	Publication	Yordan Garbatov, C. Guedes Soares. "Innovation in the Analysis and Design of Ma...	<1%

11	Internet	openaccess.hacettepe.edu.tr:8080	<1%
12	Publication	Carl E. Jacobson. "Using AutoCAD for descriptive geometry exercises", Computers...	<1%
13	Publication	Evgeni Mokrov, Konstantin Samouylov. "Performance Assessment and Compariso...	<1%
14	Publication	Xiang Liu, Jing Xu, Hongying Tang. "Analysis of Frequency-Dependent Line-of-Sig...	<1%
15	Internet	nodai.repo.nii.ac.jp	<1%
16	Publication	Arias, Juan David Pabon. "Optimal Deployment of Air Vehicle as Communication R...	<1%
17	Publication	Harpreet S. Dhillon, Vishnu Vardhan Chetlur. "Poisson Line Cox Process", Springer...	<1%
18	Internet	users.stat.umn.edu	<1%
19	Internet	honors.libraries.psu.edu	<1%
20	Internet	yorkspace.library.yorku.ca	<1%
21	Publication	Balakrishnan, Sarankumar. "Physical Layer Security in Millimeter Wave Systems: ...	<1%
22	Publication	Gaurav Duggal, R. Michael Buehrer, Jeffrey H. Reed, Nishith Tripathi. "Line-of-Sigh...	<1%
23	Publication	Jiang, Yiming. "Selected Topics in Blockchain-Aided IoT Inference.", Missouri Univ...	<1%
24	Publication	Liu, Dantong, Yue Chen, Kok Keong Chai, and Tiankui Zhang. "Backhaul aware joi...	<1%

25	Publication	Marco Giordani, Mattia Rebato, Andrea Zanella, Michele Zorzi. "Coverage and Con...	<1%
26	Publication	Thangaprakash Sengodan, Sanjay Misra, M Murugappan. "Advances in Electrical ...	<1%
27	Publication	Yulei Wu, Haojun Huang, Cheng-Xiang Wang, Yi Pan. "5G-Enabled Internet of Thin...	<1%
28	Internet	dagstuhl.sunsite.rwth-aachen.de	<1%
29	Internet	digital.library.unt.edu	<1%
30	Internet	research-management.mq.edu.au	<1%
31	Internet	www.frontiersin.org	<1%
32	Internet	www.qeios.com	<1%
33	Publication	Anastasia Kondratyeva, Daria Ivanova, Vyacheslav Begishev, Ekaterina Markova e...	<1%

How Long Can I Transmit? A Mobility Aware mmWave-based UAV Communication Framework

*A dissertation submitted in
partial fulfilment for the degree of*

**Master of Technology
in
Computer Science**

by

Shawon Mitra

Roll no. - CS2321

under the supervision of

Prof. Sasthi C. Ghosh

Advanced Computing and Microelectronics Unit
(ACMU)



INDIAN STATISTICAL INSTITUTE, KOLKATA

JUNE 2025

** This work has been submitted at The 33rd International Conference on
Software, Telecommunications, and Computer Networks (SoftCOM 2025), to be
held at Split, Croatia, during 18-20 September, 2025.*

Declaration

I, **Shawon Mitra**, with Roll No. **CS2321**, hereby declare that the material presented in the dissertation titled **How Long Can I Transmit? A Mobility Aware mmWave-based UAV Communication Framework** represents original work carried out by me for the degree of **Master of Technology in Computer Science** at the **Indian Statistical Institute, Kolkata**. Furthermore, I affirm that no sections of this report have been sourced or copied from external references without proper attribution. I am aware that any instances of plagiarism or the use of unacknowledged materials from third parties will be treated with the utmost seriousness and consequences.

Shawon Mitra.

Shawon Mitra
M.Tech (CS), CS2321
Indian Statistical Institute
Kolkata 700108, India

CERTIFICATE

This is to certify that the dissertation titled **How Long Can I Transmit? A Mobility Aware mmWave-based UAV Communication Framework** submitted by **Shawon Mitra** to the **Indian Statistical Institute, Kolkata**, in partial fulfillment of the requirements for the degree of **Master of Technology in Computer Science**, is an authentic and genuine record of the research work carried out by the candidate under my supervision and guidance. I affirm that the dissertation has met all the necessary requirements in accordance with the regulations of this institute.



Prof. Sasthi C. Ghosh
Advanced Computing and Microelectronics Unit
Indian Statistical Institute
Kolkata 700108, India

Acknowledgement

I extend my sincere gratitude to **Prof. Sasthi C. Ghosh**, my advisor at the Advanced Computing and Microelectronics Unit of the Indian Statistical Institute in Kolkata, for his invaluable guidance, encouragement, and support throughout the course of this work. His expertise and insightful feedback have been instrumental in shaping this research.

I am deeply grateful to all the teachers at the Indian Statistical Institute for their invaluable advice, insight, and instruction, which provided a crucial perspective to my research. Special thanks go to Dr. Subhojit Sarkar and all the other seniors for their constant mentoring.

Finally, I want to express my gratitude to my parents and extended family for their unwavering support. I also extend my sincere appreciation to all my friends for their continuous assistance and encouragement. I am thankful to everyone who has contributed to my growth and success, even if I have inadvertently missed mentioning them on the above list.

Abstract

32 One primary focus of next generation wireless communication networks is the millimeterwave (mmWave) spectrum, typically considered in the 30 GHz to 300 GHz frequency range. Despite their promise of high data rates, mmWaves suffers from severe attenuation while passing through obstacles. Unmanned aerial vehicles (UAVs) have been proposed to offset this limitation on account of their additional degrees of freedom, which can be leveraged to provide line of sight (LoS) transmission paths. While some prior works have proposed analytical frameworks to compute the LoS probability for static ground users and a UAV, the same is lacking for mobile users on the ground. 20 In this thesis, we consider the popular Manhattan point line process (MPLP) to model an urban environment, and a ground user mobility model similar to Manhattan mobility model. We give 23 closed form expression for the expected duration of LoS between a static UAV in the air and a mobile ground user, and validate the same through simulations. 26 To demonstrate the efficacy of the proposed analysis, we propose a simple user association algorithm that greedily assigns the UAVs to users with the highest expected LoS time, and show that it outperforms the existing benchmark schemes that assign the users to the nearest UAVs with LoS.

Keywords

5G, UAV, mmWave communication, stochastic geometry, Expected LoS time, user-UAV association

Contents

Declaration	ii
Acknowledgement	iv
Abstract	v
1 Introduction	1
2 System Model	4
2.1 LoS Probability for Static User	6
3 Mathematical Analysis	8
3.1 Expected LoS Time	8
3.2 UAV association	15
4 Simulation Results	16
5 Conclusion	21

6

List of Figures

2.1	Considered urban environment: Top view	4
2.2	Considered urban environment: Side view (LoS and Non-LoS) . .	5
3.1	User movement along X-axis (User-UAV link)	9
3.2	Proof of Lemma 3.1.1	10
4.1	UAV heights vs expected LoS time	17
4.2	Building ratio vs expected LoS time	18
4.3	Velocity vs expected LoS time	19
4.4	Time under LoS for existing and proposed schemes	20

Chapter 1

Introduction

Though primarily developed with the military in mind, civilian utilities of unmanned aerial vehicles (UAVs) have seen a sharp rise in recent years. From aerial mapping to smart agriculture, from package delivery to drone shows, the opportunities are limitless. As the world becomes more and more connected, UAVs are poised to be an important enabling technology for next generation communication networks [1, 2]. Typical use cases of UAVs in the wireless communication scenario involve increasing the coverage area, relaying, and collection of delay tolerant information from low power sensing devices [3]. Among these, of particular interest is the first one, providing coverage to terrestrial users from the air. UAVs can come to the rescue if the terrestrial infrastructure becomes incapable of providing service, either due to damage [4] or sudden spatial spike in user demand [5]. Their fast, on-demand deployability pitches them as ideal candidates for short time periods.

Spatial flexibility offered by these UAVs are of special interest in millimeter-wave (mmWave) communications [6]. Millimeterwave communications have seen tremendous interest over the last decade, fuelled by their promise of large bandwidth, and communication in the gigabits per second (Gbps) rates [7]. The increase in bandwidth hungry applications like full HD streaming, and virtual reality has led to further interest in the field. However, in spite of the high bandwidth, and the subsequent high speeds provided by mmWaves, they have some inherent drawbacks. Communication over these low wavelength signals are extremely prone to blockages [8]. This problem is especially exacerbated in urban

scenarios, where the dense distribution of buildings causes a significant number of links to be blocked. Measurements show that the penetration loss caused due to a building can be as high as 40dB [7], which causes noticeable degradation in quality of service. Consequently, mmWave can provide high data rates only if the UAV is line of sight (LoS) from the user [8]. It is no wonder thus, that computation of the LoS probability between the user and the UAV is an important problem.

Considerable work has been done to capture the LoS probability in wireless networks, most of which leverages stochastic geometry. The benefit of stochastic models when compared to ray tracing methods like [9] is that they are computationally cheaper, and produces faster network evaluation with acceptable accuracy [10]. A few models have been proposed by 3GPP[11] and ITU [12] to consider the LoS probability of wireless communication systems deployed in urban scenarios. A Poisson point process (PPP) was used in [13] to model the locations of terrestrial base stations, and subsequently provide a tractable closed form expression on coverage probability. A similar coverage analysis was done for mmWave networks in [14], where the base stations were considered to form a PPP with a fixed density. While the previous works dealt with 2D distributions of base stations, [15] additionally considered the heights of the transmitters and receivers to be drawn from the exponential distribution, to compute the blockage effects in 3D. Using concepts from random shape theory, authors in [16] proposed an analytical framework for LoS probability for an environment with buildings deployed irregularly. Regular urban grids have also been considered while computing the LoS probability. Authors in [17] modelled an urban grid, with roads and buildings generated using the Manhattan Poisson line process (MPLP) featuring two homogenous PPPs. Closed form LoS probability expressions were provided by authors in [18] using different building height distributions. A similar study was done in [19], where an urban tactical mmWave network was considered with a fleet of UAVs, and a vehicle on the ground. Leveraging tools from stochastic geometry, a closed form expression for the LoS connectivity probability was proposed.

One noticeable thing in the previous works is the absence of user mobility, *i.e.*, they consider the ground user to be static during a small time epoch, while computing the LoS probability. As a result, they disregard the fact that a user experiencing LoS with the UAV at the start of a time interval does not always have an LoS throughout the entire duration of the interval. In an urban environment,

8
22
2
3
6
21
6

the presence of buildings will cause intermittent blockages of the mmWave links, thereby leading to network inefficiencies. In this thesis, we propose an analytical method to model the expected time under LoS for a mobile ground user connected with a UAV. More precisely, we consider that the user is moving in accordance with a mobility model while communicating with a UAV. Considering an urban grid environment, we first consider the LoS probability assuming that the user is static, and then incorporate mobility. We thereafter compute the expectation of the time under LoS from first principles. Two cases arise, for one of which we find a closed form expression, while for the other, we use Simpson's 1/3 rule to get an approximate solution. We finally incorporate the two together to propose an analytical expression that gives us the expected LoS time a user has with a static UAV in an urban environment. To show the utility of this metric, we propose a greedy algorithm to maximally associate mobile users with UAVs, with an aim to increase their expected LoS time, and show the superiority of our approach compared to an existing benchmark scheme as commonly used in [20, 21, 22] that greedily assigns the user to the nearest UAV providing LoS to it. To the best of our knowledge, this is the first work that attempts to model the expected time under LoS for a mobile ground user using tools from stochastic geometry, and proposes a user association algorithm based on this expected LoS time.

6

The rest of the thesis is arranged as follows. Chapter 2 details the system model, while the analysis and the user association are done in Chapter 3. The proposed models are validated through simulation and compared with the existing works in Chapter 4. We conclude in Chapter 5.

Chapter 2

System Model

We consider the following urban layout model as in [18, 19]. Roads run orthogonally, either along the X-axis from east to west, or along the Y-axis from north to south. The starting locations of the buildings are drawn from an MPLP, which basically comprises two independent homogeneous PPPs X and Y each with density λ . The region between two consecutive points on an axis contains a road, and a building block as shown in Fig. 2.1. The mean street and building widths are considered to be μ_s and μ_b respectively, while $\lambda = \frac{1}{\mu_s + \mu_b}$. Along each axis, the ratio of the building widths is $\frac{\mu_b}{\mu_b + \mu_s}$, while the ratio of street widths is $\frac{\mu_s}{\mu_b + \mu_s}$ with respect to the total length.

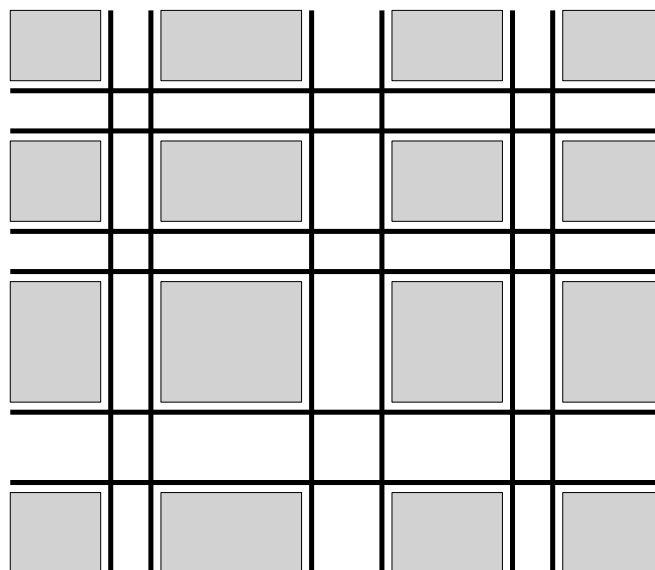


Figure 2.1: Considered urban environment: Top view

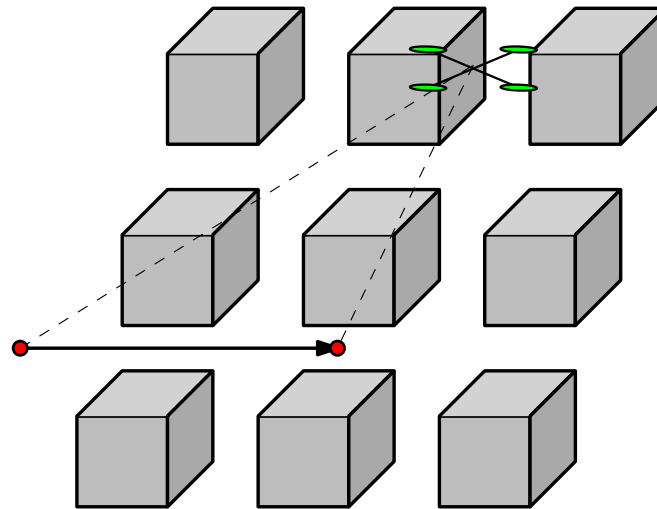


Figure 2.2: Considered urban environment: Side view (LoS and Non-LoS)

4 It is assumed that each non-road section comprises a single building, whose height is a random variable H_B and $F_{H_B}(h)$ is the cumulative distribution function (CDF) of the building height. Since we are dealing entirely with communications in the mmWave range, we consider building walls to be thick enough to cause sufficient signal attenuation to cause link failure. In other words, anything other than optical LoS is considered as a failed path (non-LoS). As in Fig. 2.2, the 3D path is occluded only when 1) the 2D projection of the transmission path crosses a building side, and 2) the height of the said building is greater than the height of the transmission path at the point of 2D intersection. For analysis, we assume without loss of generality that the user is at ground level, initially at $(0, 0, 0)$, and that a single UAV is flying at fixed 3D coordinates (x_u, y_u, h_u) . The user is moving with a fixed velocity v along a road, which again without loss of generality can be considered to be along the positive X-axis. The user moves with the chosen velocity with no change in direction for a small time interval $[0, T]$. The case of a direction change during the time interval $[0, T]$ will be considered in a subsequent future work and is thus out of scope of the current thesis.

13

33

3

8

27

2.1 LoS Probability for Static User

Here assuming that the user remains static during the time interval $[0, T]$, we compute the LoS probability between the user and the UAV. The positions of the user and the UAV are $\hat{g}_0 = (x_0, y_0, 0)$, $\hat{u} = (x_u, y_u, h_u)$, respectively, and the width of the street containing the user is w . Without loss of generality, we can consider the UAV to be at either first or second quadrants. Based on this scenario, the following formula (2.1) can provide the probability of the LoS between the user and the UAV, as in [18].

$$P_{LoS}(\hat{g}_0, \hat{u}) = P_{LoS}^0(\hat{g}_0, \hat{u}) \cdot P_{LoS}^X(\hat{g}_0, \hat{u}) \cdot P_{LoS}^Y(\hat{g}_0, \hat{u}) \quad (2.1)$$

$P_{LoS}^0(\hat{g}_0, \hat{u})$ is the probability that the height of the nearest contact building along the projected LoS link is lower than the LoS height, $h_1(\hat{c}, \hat{g}_0, \hat{u})$, at the point of intersection $\hat{c} = (\tilde{x}, \tilde{y})$, i.e.,

$$P_{LoS}^0 = P(H_B \leq h_1(\hat{c}, \hat{g}_0, \hat{u})) = F_{H_B}(h_1(\hat{c}, \hat{g}_0, \hat{u})) \quad (2.2)$$

where H_B is the height of the nearest contact building and

$$h_1(\hat{c}, \hat{g}_0, \hat{u}) = \frac{|\tilde{x} - x_0|}{|x_u - x_0|} h_u = \frac{|\tilde{y} - y_0|}{|y_u - y_0|} h_u. \quad (2.3)$$

P_{LoS}^X, P_{LoS}^Y are the void probabilities of two non-homogeneous PPPs along the X and Y axes in the interval $[\tilde{x}, x_u]$ and $[\tilde{y}, y_u]$ respectively, i.e.,

$$P_{LoS}^X = \exp\left(-\lambda \int_{\tilde{x}}^{x_u} [1 - F_{H_B}(h^x(x, \hat{g}_0, \hat{u}))] dx\right) \quad (2.4)$$

$$P_{LoS}^Y = \exp\left(-\lambda \int_{\tilde{y}}^{y_u} [1 - F_{H_B}(h^y(y, \hat{g}_0, \hat{u}))] dy\right) \quad (2.5)$$

where h^x and h^y are the LoS heights at $(x, 0)$ and $(0, y)$ respectively and

$$h^x(x, \hat{g}_0, \hat{u}) = \frac{|x - x_0|}{|x_u - x_0|} h_u, \quad (2.6)$$

$$h^y(y, \hat{g}_0, \hat{u}) = \frac{|y - y_0|}{|y_u - y_0|} h_u. \quad (2.7)$$

Now, let the height of the building follow Rayleigh distribution with parameter σ ($H_B \sim \text{Rayleigh}(\sigma)$), the equations (2.2), (2.4), (2.5) will be,

$$P_{LoS}^0 = \left[1 - \exp\left(-\frac{h_1(\hat{x}_0, \hat{u})^2}{2\sigma^2}\right) \right] \quad (2.8)$$

$$P_{LoS}^X = \exp\left(-\lambda \int_{\tilde{x}}^{x_u} \exp\left(-\frac{h^x(x, \hat{x}_0, \hat{u})^2}{2\sigma^2}\right) dx\right) \quad (2.9)$$

$$P_{LoS}^Y = \exp\left(-\lambda \int_{\tilde{y}}^{y_u} \exp\left(-\frac{h^y(y, \hat{x}_0, \hat{u})^2}{2\sigma^2}\right) dy\right) \quad (2.10)$$

Using (2.3), (2.6), (2.7) (2.8), (2.9) and (2.10), we can rewrite (2.1) as

$$P_{LoS}(\hat{g}_0, \hat{u}) = \left[1 - \exp\left(-\frac{h_u^2}{2\sigma^2} \frac{|\tilde{x} - x_0|^2}{|x_u - x_0|^2}\right) \right] \times \exp\left(A|x_u - x_0| + B|y_u - y_0|\right) \quad (2.11)$$

where A and B have the following expressions

$$A = -\lambda \sqrt{\frac{\pi}{2}} \frac{\sigma}{h_u} \left[\operatorname{erf}\left(\frac{h_u}{\sqrt{2}\sigma}\right) - \operatorname{erf}\left(\frac{h_u}{\sqrt{2}\sigma} \frac{|\tilde{x} - x_0|}{|x_u - x_0|}\right) \right]$$

$$B = -\lambda \sqrt{\frac{\pi}{2}} \frac{\sigma}{h_u} \left[\operatorname{erf}\left(\frac{h_u}{\sqrt{2}\sigma}\right) - \operatorname{erf}\left(\frac{h_u}{\sqrt{2}\sigma} \frac{|\tilde{y} - y_0|}{|y_u - y_0|}\right) \right]$$

where $\operatorname{erf}(z) = \frac{2}{\sqrt{\pi}} \int_0^z \exp(-t^2) dt$.

Chapter 3

Mathematical Analysis

Here, we consider the scenario where the user is not static. Since we consider an urban layout, the buildings will occlude allocated links, thereby causing intermittent link failures due to user mobility. First, in section 3.1, we derive an expression of the expected LoS time of the user with a given UAV for a given time epoch $[0, T]$, based on our system model. Here we assume that the time epoch T is small, so that the user does not change its direction and the velocity v during $[0, T]$. Then, in section 3.2, we derive a user association policy where a user is associated with the UAV providing the highest expected LoS time.

3.1 Expected LoS Time

Let the user move with velocity v along the positive X-axis, the buildings are placed according to the PPP with parameter λ , and the building heights are drawn from a Rayleigh distribution with parameter σ (Fig. 3.1). Let $\hat{g}_t = (x_t, y_t)$ be the position of the user at time $t \in [0, T]$. Our motivation is to track the projected LoS path at any time t to calculate the LoS probability of the user with the UAV. We know from (2.11) that the LoS probability depends on the coordinates of the first intersecting sides of the building and it alters over time due to the mobility of the user. With time, the sides are alternatively changing to a side parallel to the X-axis and then parallel to the Y-axis and vice versa.

Let us first assume that the projected LoS path does not alter the first intersecting side parallel to the X-axis during the time interval $[0, T_\alpha]$. Under this assumption,

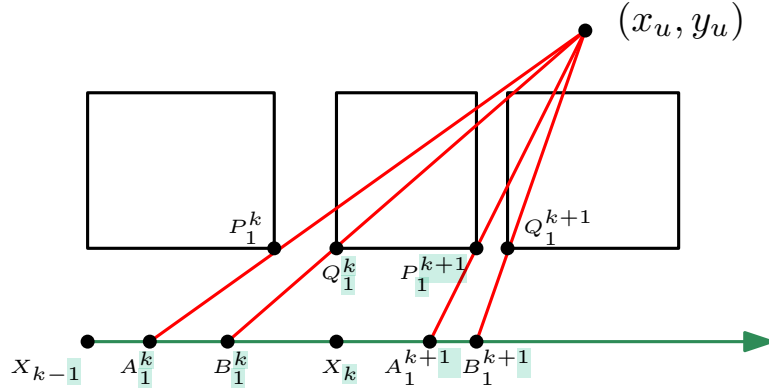


Figure 3.1: User movement along X-axis (User-UAV link)

the following lemma 3.1.1 gives an expression of the LoS probability at any time $t \in [0, T_\alpha]$ and also a closed form expression of the expected LoS time for the user in this time interval.

Lemma 3.1.1. *Let the first intersecting side of a projected LoS link be parallel to the X-axis, which does not change over the time interval $[0, T_\alpha]$. The LoS probability of the user at any time $t \in [0, T_\alpha]$, will be*

$$P_{LoS}(\hat{g}_t, \hat{u}) = P_{LoS}(\hat{g}_0, \hat{u}) \times \exp(Avt) \quad (3.1)$$

where $P_{LoS}(\hat{g}_0, \hat{u})$ is the initial LoS probability between the user and the UAV as in (2.11). The expected LoS time $E[T_{LoS}(0, T_\alpha)]$ of the user in this interval $[0, T_\alpha]$ will be,

$$E[T_{LoS}(0, T_\alpha)] = P_{LoS}(\hat{g}_0, \hat{u}) \times \frac{1}{Av} (\exp(AvT_\alpha) - 1) \quad (3.2)$$

Proof: Let the user be at $\hat{g}_0 = (x_0, y_0)$ at $t = 0$ and then starts moving with velocity v along the positive X-axis. At time $t \in [0, T_\alpha]$, let the new location of the user be $\hat{g}_t = (x_t, y_t)$. Thus, $x_t = x_0 + vt$ and $y_t = y_0$. Now, let $(\tilde{x}_t, \tilde{y}_t)$ be the coordinates of first point of intersection of the projected LoS link with the building after time $t \in [0, T_\alpha]$. So, using (2.11), the LoS probability of the user at time $t \in [0, T_\alpha]$ is

$$P_{LoS}(\hat{g}_t, \hat{u}) = \left[1 - \exp\left(-\frac{h_u^2}{2\sigma^2} \frac{|\tilde{x}_t - x_t|^2}{|x_u - x_t|^2}\right) \right] \times \exp\left(A'|x_u - x_t| + B'|y_u - y_t|\right) \quad (3.3)$$

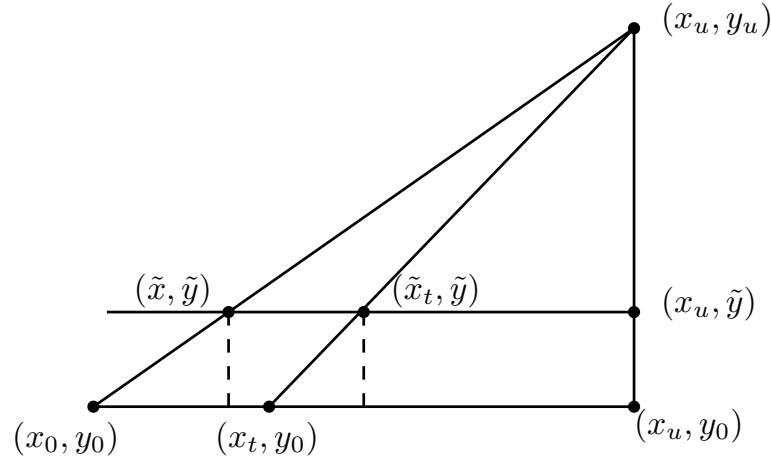


Figure 3.2: Proof of Lemma 3.1.1

where

$$A' = -\lambda \sqrt{\frac{\pi}{2}} \frac{\sigma}{h_u} \left[\operatorname{erf}\left(\frac{h_u}{\sqrt{2}\sigma}\right) - \operatorname{erf}\left(\frac{h_u}{\sqrt{2}\sigma} \frac{|\tilde{x}_t - x_t|}{|x_u - x_t|}\right) \right]$$

$$B' = -\lambda \sqrt{\frac{\pi}{2}} \frac{\sigma}{h_u} \left[\operatorname{erf}\left(\frac{h_u}{\sqrt{2}\sigma}\right) - \operatorname{erf}\left(\frac{h_u}{\sqrt{2}\sigma} \frac{|\tilde{y}_t - y_t|}{|y_u - y_t|}\right) \right].$$

Here, $\tilde{x}_t = \tilde{x} + \frac{|y_u - \tilde{y}|}{|y_u - y|} vt$ and $\tilde{y}_t = \tilde{y}$. Again, from Fig. 3.2,

$$\frac{|\tilde{y}_t - y_t|}{|y_u - y_t|} = \frac{|\tilde{x}_t - x_t|}{|x_u - x_t|} = \frac{|\tilde{y} - y_0|}{|y_u - y_0|} = \frac{|\tilde{x} - x_0|}{|x_u - x_0|}, \quad (3.4)$$

which implies $P_{LoS}^0(\hat{g}_t, \hat{u})$ at any time t , $0 < t \leq T_\alpha$, is the same as P_{LoS}^0 at $t = 0$ as obtained in (2.8). This in turn implies that $A' = B' = A = B$ for all $t \in [0, T_\alpha]$. Hence the LoS probability $P_{LoS}(\hat{g}_t, \hat{u})$ of the user at time $t \in [0, T_\alpha]$ given by equation (3.3) can be rewritten as,

$$\begin{aligned} &= P_{LoS}^0(\hat{g}_0, \hat{u}) \exp\left(A'|x_t - x_u| + B'|y_t - y_u|\right) \\ &= P_{LoS}^0(\hat{g}_0, \hat{u}) \exp\left(A|x_0 + vt - x_u| + B|y_0 - y_u|\right) \\ &= P_{LoS}^0(\hat{g}_0, \hat{u}) \exp\left(A|x_0 - x_u| + B|y_0 - y_u| + Avt\right) \\ &= P_{LoS}(\hat{g}_0, \hat{u}) \times \exp(Avt) \text{ (Using (2.11))} \end{aligned}$$

By integrating this expression with respect to t in $[0, T_\alpha]$, we will get the expected LoS time of the user in $[0, T_\alpha]$ as,

$$\begin{aligned} E[T_{LoS(0, T_\alpha)}] &= \int_0^{T_\alpha} P_{LoS}(\hat{g}_t, \hat{u}) dt \\ &= \int_0^{T_\alpha} P_{LoS}(\hat{g}_0, \hat{u}) \times \exp(Avt) dt \\ &= P_{LoS}(\hat{g}_0, \hat{u}) \times \frac{1}{Av} (\exp(AvT_\alpha) - 1) \quad \square \end{aligned}$$

Now we consider the case where the LoS link is first blocked by the side of a building block parallel to the Y axis, and it does not change during the time interval $[0, T_\beta]$. The following lemma 3.1.2 will give the expression for the expected LoS time in the time interval $[0, T_\beta]$.

Lemma 3.1.2. *The expected LoS time $E[T_{LoS(0, T_\beta)}]$ of the user in the time interval $[0, T_\beta]$ is*

$$\begin{aligned} &= \int_0^{T_\beta} P_{LoS}(\hat{g}_t, \hat{u}) dt \\ &\approx \frac{T_\beta}{6} \left[P_{LoS}(\hat{g}_0, \hat{u}) + 4P_{LoS}(\hat{g}_{\frac{T_\beta}{2}}, \hat{u}) + P'_{LoS}(\hat{g}_{T_\beta}, \hat{u}) \right] \end{aligned} \quad (3.5)$$

Proof: The proof goes along similar lines as that of Lemma 3.1.1. However, in this case, for any $t \in [0, T_\beta]$, we get $x_t = x_0 + vt$, $y_t = y_0$, $\tilde{x}_t = \tilde{x}$, $\tilde{y}_t = \tilde{y} - \frac{|y_u - y|}{|x_u - x|} vt$. Hence the LoS probability $P_{LoS}(\hat{g}_t, \hat{u})$ of the user at time $t \in [0, T_\beta]$ given by equation (3.3) can be rewritten as,

$$\begin{aligned} P_{LoS}(\hat{g}_t, \hat{u}) &= \left[1 - \exp\left(-\frac{h_u^2 |\tilde{x} - x_0 - vt|^2}{2\sigma^2 |x_u - x_0 - vt|^2}\right) \right] \\ &\quad \times \exp\left(A'' |x_u - x_0 - vt| + B'' |y_u - y_0|\right), \end{aligned} \quad (3.6)$$

where

$$A'' = -\lambda \sqrt{\frac{\pi}{2}} \frac{\sigma}{h_u} \left[\operatorname{erf}\left(\frac{h_u}{\sqrt{2}\sigma}\right) - \operatorname{erf}\left(\frac{h_u}{\sqrt{2}\sigma} \frac{|\tilde{x} - x_0 - vt|}{|x_u - x_0 - vt|}\right) \right]$$

$$B'' = -\lambda \sqrt{\frac{\pi}{2}} \frac{\sigma}{h_u} \left[\operatorname{erf}\left(\frac{h_u}{\sqrt{2}\sigma}\right) - \operatorname{erf}\left(\frac{h_u}{\sqrt{2}\sigma} \frac{|\tilde{y} - \frac{|y_u - y|}{|x_u - x|} vt - y_0|}{|y_u - y_0|}\right) \right].$$

In this case, no similar closed form expression of $P_{LoS}(\hat{g}_t, \hat{u})$ like (3.1) is obtained as the ratio given by (3.4) does not hold. It also implies that $A'' \neq B''$ for any value $x_0 \leq x_t \leq x_0 + vT_\beta$. So, to calculate the expected LoS time $E[T_{LoS(0, T_\beta)}] = \int_0^{T_\beta} P_{LoS}(\hat{g}_t, \hat{u}) dt$ of the user in $[0, T_\beta]$, we use Simpson's 1/3-Rule to get (3.5). \square

So far we have computed the expected time under LoS for two scenarios, viz. when the LoS link is first blocked by the side of the building parallel to the X and Y-axes, respectively. However, as the user moves along its path, these two events will happen alternatively, throughout the epoch of time considered $[0, T]$. Let $A_1^1, B_1^1; A_1^2, B_1^2; \dots; A_1^k, B_1^k$ be the user positions on the roads where the projected LoS link changes its first intersecting sides and $t_A^1, t_B^1; t_A^2, t_B^2; \dots; t_A^k, t_B^k$ be their respective time points. Our main objective would thus be to consider the sum of expected LoS time for all such intervals. For each such interval, we can compute the expected LoS time using Lemma 3.1.1 and Lemma 3.1.2, respectively.

Consider $\hat{x}_1, \hat{x}_2, \dots, \hat{x}_k$ are the x coordinates of the points drawn from the MPLP. Let $P_1^1, Q_1^1; P_1^2, Q_1^2; \dots; P_1^k, Q_1^k$ be the left and right corner points of the buildings.

From Fig. 3.1,

$$Q_1^k = \hat{x}_k, \quad (3.7)$$

$$P_1^k = \lambda |\hat{x}_k \mu_b + \hat{x}_{k-1} \mu_s|, \quad (3.8)$$

$$\frac{y_u}{x_u - A_1^k} = \frac{y_u - w}{x_u - P_1^k}, \quad (3.9)$$

$$\frac{y_u}{x_u - B_1^k} = \frac{y_u - w}{x_u - Q_1^k}. \quad (3.10)$$

By solving the above equations, we get

$$A_1^k = \frac{y_u P_1^k - w x_u}{y_u - w}, \quad B_1^k = \frac{y_u Q_1^k - w x_u}{y_u - w}, \quad (3.11)$$

where w is the known street width. So $t_A^k = \frac{A^k}{v}$ & $t_B^k = \frac{B^k}{v}$. Now, we calculate $E[T_{LoS(0,T)}]$ for the given time interval $[0, T]$ in the following **Theorem 3.1.3**.

Theorem 3.1.3. *Let there be ℓ event points in between the time interval $[0, T]$. So, the total LoS time of the user will be,*

$$E[T_{LoS(0,T)}^\ell] = E[T_{LoS(0,t_A^1)}] + \sum_{i=1}^{\ell} E[T_{LoS(t_A^i, t_B^i)}] + \sum_{i=1}^{\ell-1} E[T_{LoS(t_B^i, t_A^{i+1})}] + E[T_{LoS(t_B^\ell, T)}] \quad (3.12)$$

Proof: Let the user crosses ℓ intersections during $[0, T]$. So, there will be ℓ pairs of A_i^i and B_i^i in $[0, T]$. At each A_i^i and B_i^i , the projected LoS link will alter. Hence,

$$\begin{aligned} E[T_{LoS(0,T)}^\ell] &= \int_0^T P_{LoS}(\hat{g}_t, \hat{u}) dt \\ &= \int_0^{t_A^1} P_{LoS}(\hat{g}_t, \hat{u}) dt + \sum_{i=1}^{\ell} \int_{t_A^i}^{t_B^i} P_{LoS}(\hat{g}_t, \hat{u}) dt + \dots \\ &\quad + \sum_{i=1}^{\ell-1} \int_{t_B^i}^{t_A^{i+1}} P_{LoS}(\hat{g}_t, \hat{u}) dt + \int_{t_B^\ell}^T P_{LoS}(\hat{g}_t, \hat{u}) dt \\ &= E[T_{LoS(0,t_A^1)}] + \sum_{i=1}^{\ell} E[T_{LoS(t_A^i, t_B^i)}] \\ &\quad + \sum_{i=1}^{\ell-1} E[T_{LoS(t_B^i, t_A^{i+1})}] + E[T_{LoS(t_B^\ell, T)}] \quad \square \end{aligned}$$

The number of event points are drawn from PPP and hence ℓ is not fixed in $[0, T]$. In the following theorem we first calculate the probability of the highest number of events that can occur in $[0, T]$ and then compute the expected LoS time in $[0, T]$.

Theorem 3.1.4. *If N is the highest number of events that occur in $[0, T]$ with probability $(1 - \epsilon)$, then the expected total LoS time of the user will be,*

$$E[T_{LoS}] = \frac{\sum_{\ell=0}^N E[T_{LoS}^\ell] \times \frac{(\lambda v T)^\ell e^{-\lambda v T}}{\ell!}}{\sum_{\ell=0}^N \frac{(\lambda v T)^\ell e^{-\lambda v T}}{\ell!}} \quad (3.13)$$

Proof : Let the user be at \hat{g}_0 and move with velocity v along the X-axis in $[0, T]$. Let \mathcal{N} be the random variable that counts the number of events that occur in $[0, T]$. Clearly it follows a Poisson distribution with parameter $\lambda v T$. So, the highest number of events N that can occur in $[0, T]$ with probability $1 - \epsilon$ will be,

$$P(\mathcal{N} \leq N) \geq 1 - \epsilon \implies P(\mathcal{N} \geq N) \leq \epsilon \quad (3.14)$$

Therefore, the value of N will be,

$$N = \min \left\{ n \in \mathbb{N} : \sum_{j=0}^n \frac{\mu^j e^{-\mu}}{j!} \geq 1 - \epsilon \right\} \quad (3.15)$$

where $\mu = \lambda v T$.

Now for each ℓ , $0 \leq \ell \leq N$, $E[T_{LoS(0,T)}^\ell]$, the expected LoS time of the user in $[0, T]$, can be obtained by (3.12). The total expected LoS time $E[T_{LoS(0,T)}]$ can be calculated using the weighted average for all ℓ where each weight w_ℓ denotes the probability that ℓ number of events occur in $[0, T]$. So,

$$E[T_{LoS(0,T)}] = \frac{\sum_{\ell=0}^N w_\ell E[T_{LoS(0,T)}^\ell]}{\sum_{\ell=0}^N w_\ell}$$

where $w_\ell = \frac{(\lambda v T)^\ell e^{-\lambda v T}}{\ell!}$. □

3.2 UAV association

Using the expected LoS time computed in Theorem 3.1.4, we derive a greedy user association algorithm that associates a user with the UAV that provides the maximum expected LoS time to it. Depending on the initial transmission distance and the user velocity, a user may not remain inside the UAV coverage area for the entire interval $[0, T]$. If we consider a UAV at height h_u , with a maximum 3D transmission distance of d_{3D} , the 2D coverage radius of the UAV becomes $\sqrt{d_{3D}^2 - h_u^2}$. Obviously, the time T' a user will spend within this coverage radius of the UAV depends on v , which might be less than T . Let T_{min} be the minimum of T' and T . Thus we shall calculate the expected LoS time of the user associated with the UAV under consideration during the time interval $[0, T_{min}]$. We compare our derived association policy with existing approaches like [20, 21, 22] that associate a user to the nearest UAV providing the LoS. However, in this existing approach, it is assumed that the user remains static over the entire interval $[0, T]$. We reiterate that the LoS at the beginning of the interval does not necessarily imply that this LoS will be maintained throughout the interval. In our approach, we have computed the expected LoS time considering user mobility.

Algorithm 1: User Association

Data: $\mathcal{U}, \mu_b, \mu_s, \lambda, \sigma, v, T, d_{3D}, \epsilon$

Result: u

$N \leftarrow f(\lambda, v, T, \epsilon)$ **for** $u \in \mathcal{U}$ **do**

$T' \leftarrow \frac{U_x^+ \sqrt{d_{3D}^2 - U_h^2 - U_y^2}}{v}$
 $T \leftarrow \min(T', T)$
 $E[T_{LoS}^u] \leftarrow \text{LoSTime}(\mu_b, \mu_s, \sigma, v, T, N)$

end

$u \leftarrow \underset{u \in \mathcal{U}}{\text{argmax}} E[T_{LoS}^u]$

Chapter 4

Simulation Results

In this section, we evaluate the numerical results for the expressions derived throughout the thesis and validate the same using Monte Carlo simulations. We start by studying the correctness of our model by executing it in a variety of environments. Finally, we compare the proposed user association approach with an existing one [20, 21, 22], and show the superiority in terms of time under LoS. We consider three distinct urban grids, namely suburban, urban, and dense urban, with parameters as provided in [23], to generate our environment. The parameters are given in Table 4.1.

Type	Mean building height	Mean building width	Mean street width
Suburban	10m	37m	10m
Urban	19m	45m	13m
Dense urban	25m	60m	20m

Table 4.1: Grid parameters based on environment selected

We consider a $400 \times 400 m^2$ region and create a grid by two MPLPs, whose parameters are drawn from Table 4.1. The heights of the buildings are assumed to be drawn from a Rayleigh distribution with parameter $\sigma = 8$. The user is initially at the origin (which can be an intersection or a road), and place a random UAV in the first or second quadrants. The user is moving with a velocity v along the positive X-axis. We use Theorem 3.1.4 to compute the expected time under LoS while considering the position of the UAV. To verify the accuracy of the results

Parameter	Value
Area	$400 \times 400 \text{ m}^2$
d_{3D}	150m
T	10s
$[v_{min}, v_{max}]$	[5, 15]m/s
$[h_{min}, h_{max}]$	[50, 350]m
ϵ	0.01

Table 4.2: Simulation parameters

obtained, we check LoS along the user trajectory using a line sweep algorithm to compute the actual LoS time. This algorithm considers a 2D triangular area enclosed by the initial and final points of the ground user, and the UAV position. We consider the environment to be known, and efficiently compute the actual LoS time. This process is repeated 10000 times and the average result is reported.

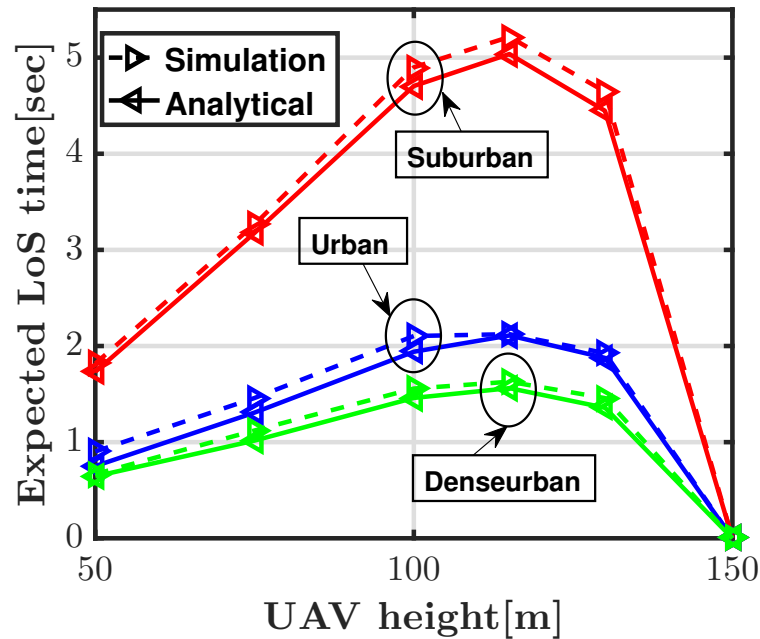


Figure 4.1: UAV heights vs expected LoS time

In Fig.4.1 we compare the analytical result with the actual time under LoS for different heights of the UAV. The initial distance between the user and the UAV is kept constant, and the user moves with velocity 15m/s along the X-axis. Increasing the height of the UAV will initially increase the expected LoS time of the user, upto a certain height determined by the coverage radius of the UAV.

Thereafter, the coverage radius criterion nullifies any gain that comes with UAV height elevation. The correctness of the proposed analysis is validated by the close fit of the experimental results with the analytical ones. As is expected, the time under LoS decreased as we move from suburban, urban, and dense urban grids.

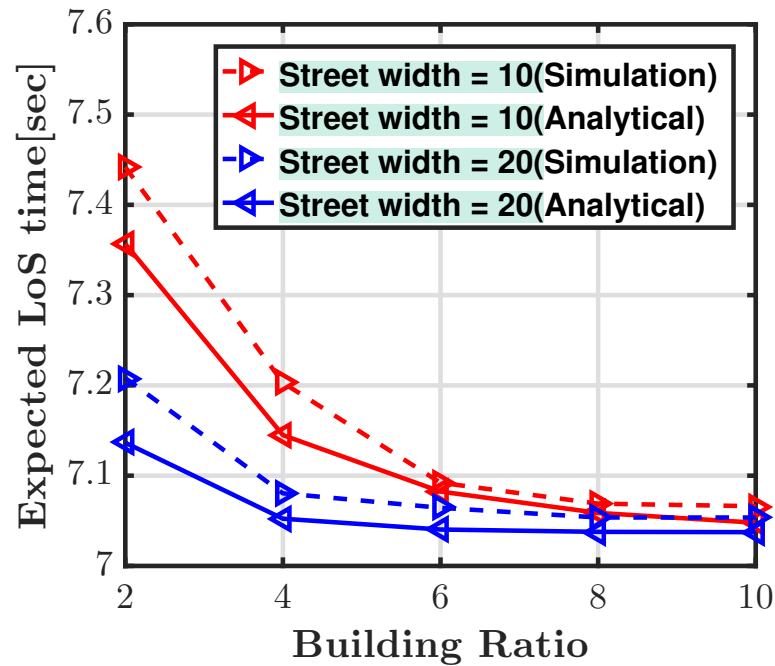


Figure 4.2: Building ratio vs expected LoS time

In Fig. 4.2 we compare the analytical result with the simulation by varying the building ratios (ratio of building width to street width) for street width 10m and 20m. Here can see both analytically and by simulation that increasing the building ratios decrease the expected LoS time, as expected. Moreover, for street width 10 the expected LoS time is greater than that for the street width 20 as the total area occupied by the buildings is much lesser in the former than the later.

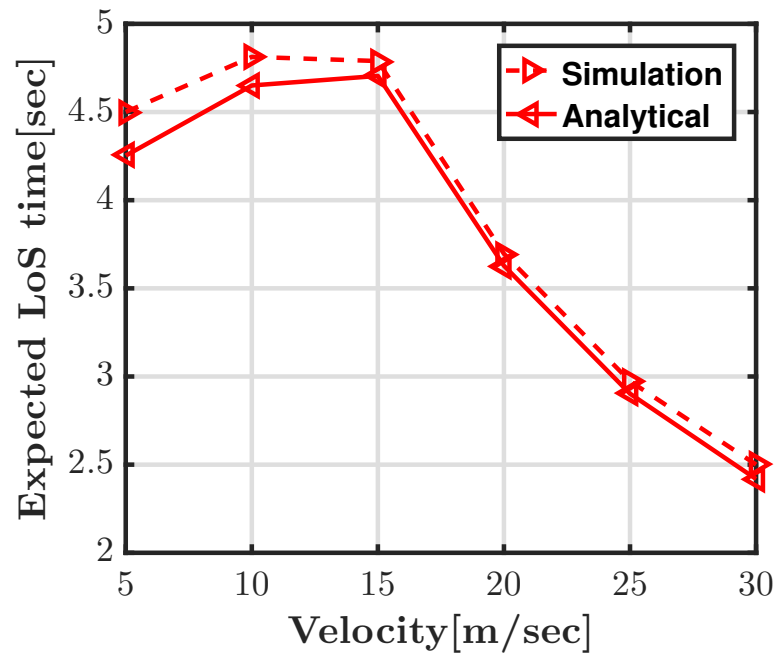


Figure 4.3: Velocity vs expected LoS time

3 In Fig. 4.3 we compare the analytical result with the simulated result for different velocities of the user. We see from the figure that increasing the velocity of the user initially increases the expected LoS time under the UAV as it travels longer distance within the coverage area of the UAV. For low velocities, a blocked user will take a long time (possibly greater than T) to get out of non-LOS, while a moderately mobile user will get out of non-LOS zone fast; hence the initial increase in expected LoS time. However, for higher velocities, the time under the UAV coverage drops fast as the user quickly goes out of range of the UAV, and hence the decreasing trend of the expected LoS time.

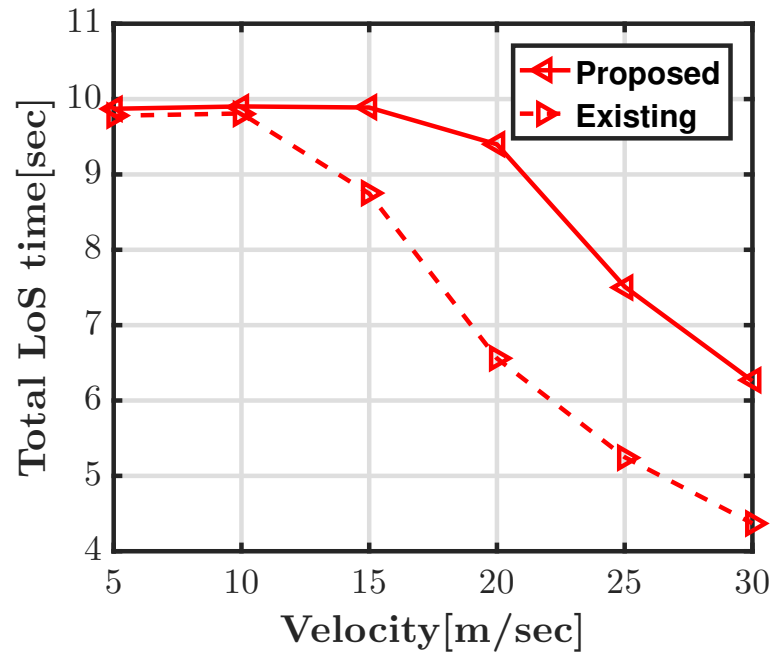


Figure 4.4: Time under LoS for existing and proposed schemes

In Fig. 4.4, we plot the total LoS time after user association by two approaches. The existing approach assigns the nearest UAV without considering user mobility, while ours prioritizes the expected LoS time considering user mobility. We fix the UAV at a height of 100m, and consider an urban environment, and plot the results by varying v . We see that at the lower velocities, the two approaches give similar results, while at higher velocities the proposed approach outperforms the existing approach by a considerable margin.

Chapter 5

Conclusion

In this thesis, we considered the often overlooked problem of time under LoS connectivity for a moving user served by UAVs. We use tools from stochastic geometry and fundamental probability to derive an analytical expression for the expected time under LoS for a mobile user on the ground in an urban scenario. Where closed form expressions are not available, we resort to approximation to get analytical results. We validate our proposed model using Monte Carlo simulations and demonstrate the utility of this metric by using it to allocate links greedily, and show its superiority compared to a existing approach. In our future work, we will incorporate non-uniform velocity of a user, with changing directions in particular, even in the small time epoch.

Bibliography

- [1] Bin Li, Zesong Fei, and Yan Zhang. “UAV Communications for 5G and Beyond: Recent Advances and Future Trends”. In: *IEEE Internet of Things Journal* 6.2 (2019), pp. 2241–2263. DOI: [10.1109/JIOT.2018.2887086](https://doi.org/10.1109/JIOT.2018.2887086).
- [2] Yongs Zeng, Qingqing Wu, and Rui Zhang. “Accessing From the Sky: A Tutorial on UAV Communications for 5G and Beyond”. In: *Proceedings of the IEEE* 107.12 (2019), pp. 2327–2375. DOI: [10.1109/JPROC.2019.2952892](https://doi.org/10.1109/JPROC.2019.2952892).
- [3] Yong Zeng, Rui Zhang, and Teng Joon Lim. “Wireless communications with unmanned aerial vehicles: opportunities and challenges”. In: *IEEE Communications Magazine* 54.5 (2016), pp. 36–42. DOI: [10.1109/MCOM.2016.7470933](https://doi.org/10.1109/MCOM.2016.7470933).
- [4] Yuntao Wang et al. “Task Offloading for Post-Disaster Rescue in Unmanned Aerial Vehicles Networks”. In: *IEEE/ACM Transactions on Networking* 30.4 (2022), pp. 1525–1539. DOI: [10.1109/TNET.2022.3140796](https://doi.org/10.1109/TNET.2022.3140796).
- [5] Jiangbin Lyu, Yong Zeng, and Rui Zhang. “UAV-Aided Offloading for Cellular Hotspot”. In: *IEEE Transactions on Wireless Communications* 17.6 (2018), pp. 3988–4001. DOI: [10.1109/TWC.2018.2818734](https://doi.org/10.1109/TWC.2018.2818734).
- [6] Chiya Zhang et al. “Research Challenges and Opportunities of UAV Millimeter-Wave Communications”. In: *IEEE Wireless Communications* 26.1 (2019), pp. 58–62. DOI: [10.1109/MWC.2018.1800214](https://doi.org/10.1109/MWC.2018.1800214).
- [7] Theodore S. Rappaport et al. “Millimeter Wave Mobile Communications for 5G Cellular: It Will Work!” In: *IEEE Access* 1 (2013), pp. 335–349. DOI: [10.1109/ACCESS.2013.2260813](https://doi.org/10.1109/ACCESS.2013.2260813).
- [8] Xiong Wang et al. “Millimeter Wave Communication: A Comprehensive Survey”. In: *IEEE Communications Surveys & Tutorials* 20.3 (2018), pp. 1616–1653. DOI: [10.1109/COMST.2018.2844322](https://doi.org/10.1109/COMST.2018.2844322).

- [9] Vasilii Semkin et al. “Characterization of Radio Links at 60 GHz Using Simple Geometrical and Highly Accurate 3-D Models”. In: *IEEE Transactions on Vehicular Technology* 66.6 (2017), pp. 4647–4656. DOI: [10.1109/TVT.2016.2617919](https://doi.org/10.1109/TVT.2016.2617919).
- [10] Xiang Liu, Jing Xu, and Hongying Tang. “Analysis of Frequency-Dependent Line-of-Sight Probability in 3-D Environment”. In: *IEEE Communications Letters* 22.8 (2018), pp. 1732–1735. DOI: [10.1109/LCOMM.2018.2842763](https://doi.org/10.1109/LCOMM.2018.2842763).
- [11] Qiuming Zhu et al. “3GPP TR 38.901 channel model”. In: *the wiley 5G Ref: the essential 5G reference online*. Wiley Press, 2021, pp. 1–35.
- [12] ITU. *Propagation Data and Prediction Methods Required for the Design of Terrestrial Broadband Radio Access Systems Operating in a Frequency Range From 3 to 60 GHz*. Tech. rep. ITU-R P.1410. ITU, Feb. 2012.
- [13] Jeffrey G. Andrews, Francois Baccelli, and Radha Krishna Ganti. “A Tractable Approach to Coverage and Rate in Cellular Networks”. In: *IEEE Transactions on Communications* 59.11 (2011), pp. 3122–3134. DOI: [10.1109/TCOMM.2011.100411.100541](https://doi.org/10.1109/TCOMM.2011.100411.100541).
- [14] Tianyang Bai and Robert W. Heath. “Coverage and Rate Analysis for Millimeter-Wave Cellular Networks”. In: *IEEE Transactions on Wireless Communications* 14.2 (2015), pp. 1100–1114. DOI: [10.1109/TWC.2014.2364267](https://doi.org/10.1109/TWC.2014.2364267).
- [15] Roman Kovalchukov et al. “Evaluating SIR in 3D Millimeter-Wave Deployments: Direct Modeling and Feasible Approximations”. In: *IEEE Transactions on Wireless Communications* 18.2 (2019), pp. 879–896. DOI: [10.1109/TWC.2018.2886188](https://doi.org/10.1109/TWC.2018.2886188).
- [16] Tianyang Bai, Rahul Vaze, and Robert W. Heath. “Analysis of Blockage Effects on Urban Cellular Networks”. In: *IEEE Transactions on Wireless Communications* 13.9 (2014), pp. 5070–5083. DOI: [10.1109/TWC.2014.2331971](https://doi.org/10.1109/TWC.2014.2331971).
- [17] François Baccelli and Xinchun Zhang. “A correlated shadowing model for urban wireless networks”. In: *2015 IEEE Conference on Computer Communications (INFOCOM)*. 2015, pp. 801–809. DOI: [10.1109/INFOCOM.2015.7218450](https://doi.org/10.1109/INFOCOM.2015.7218450).

- [18] Margarita Gapeyenko et al. “Line-of-Sight Probability for mmWave-Based UAV Communications in 3D Urban Grid Deployments”. In: *IEEE Transactions on Wireless Communications* 20.10 (2021), pp. 6566–6579. DOI: [10.1109/TWC.2021.3075099](https://doi.org/10.1109/TWC.2021.3075099).
- [19] Enass Hriba, Matthew C. Valenti, and Robert W. Heath. “Optimization of a Millimeter-Wave UAV-to-Ground Network in Urban Deployments”. In: *MILCOM 2021 - 2021 IEEE Military Communications Conference (MILCOM)*. 2021, pp. 861–867. DOI: [10.1109/MILCOM52596.2021.9653132](https://doi.org/10.1109/MILCOM52596.2021.9653132).
- [20] Nabila Sehito et al. “Optimizing User Association, Power Control, and Beamforming for 6G Multi-IRS Multi-UAV NOMA Communications in Smart Cities”. In: *IEEE Transactions on Consumer Electronics* 70.3 (2024), pp. 5702–5710. DOI: [10.1109/TCE.2024.3388596](https://doi.org/10.1109/TCE.2024.3388596).
- [21] Tianxiong Wang et al. “Performance Analysis of RIS-Assisted Large-Scale Wireless Networks Using Stochastic Geometry”. In: *IEEE Transactions on Wireless Communications* 22.11 (2023), pp. 7438–7451. DOI: [10.1109/TWC.2023.3250667](https://doi.org/10.1109/TWC.2023.3250667).
- [22] Jingxuan Chen et al. “Enhancing AIoT Device Association With Task Offloading in Aerial MEC Networks”. In: *IEEE Internet of Things Journal* 11.1 (2024), pp. 174–187. DOI: [10.1109/JIOT.2023.3300011](https://doi.org/10.1109/JIOT.2023.3300011).
- [23] Akram Al-Hourani, Sithamparanathan Kandeepan, and Simon Lardner. “Optimal LAP Altitude for Maximum Coverage”. In: *IEEE Wireless Communications Letters* 3.6 (2014), pp. 569–572. DOI: [10.1109/LWC.2014.2342736](https://doi.org/10.1109/LWC.2014.2342736).